

Orbital degeneracy and Mott transition in Mo pyrochlore oxides

Yukitoshi Motome and Nobuo Furukawa^{A,B}

Department of Applied Physics, University of Tokyo, Japan

^ADepartment of Physics and Mathematics, Aoyama Gakuin University, Japan

^BMultiferroics Project, ERATO, Japan Science and Technology Agency (JST), c/o
Department of Applied Physics, University of Tokyo, Japan

E-mail: motome@ap.t.u-tokyo.ac.jp

Abstract. We present our theoretical results on an effective two-band double-exchange model on a pyrochlore lattice for understanding intricate phase competition in Mo pyrochlore oxides. The model includes the twofold degeneracy of e'_g orbitals under trigonal field splitting, the interorbital Coulomb repulsion, the Hund's-rule coupling between itinerant e'_g electrons and localized a_{1g} spins, and the superexchange antiferromagnetic interaction between the a_{1g} spins. By Monte Carlo simulation with treating the Coulomb repulsion at an unrestricted-type mean-field level, we obtain the low-temperature phase diagram as functions of the Coulomb repulsion and the superexchange interaction. The results include four dominant phases with characteristic spin and orbital orders and the metal-insulator transitions among them. The insulating region is characterized by a 'ferro'-type orbital ordering of the e'_g orbitals along the local $\langle 111 \rangle$ axis, irrespective of the spin ordering.

1. Introduction

Mo pyrochlore oxides, whose chemical formula is generally given by $R_2\text{Mo}_2\text{O}_7$ (R is rare earth), are known to exhibit interesting phase competition and related phenomena. By chemical substitution of R cations, the system changes from a ferromagnetic metal (FM) to a spin-glass (SG) insulator systematically depending on the ionic radius of R cation [1]. On the other hand, in applied external pressure, FM collapses and turns into a peculiar paramagnetic metal (PM) with showing an intermediate SG metallic state, whereas the SG insulator remains rather robust against pressure [2]. This variety of phases and competition among them offer an opportunity to systematically study many fascinating phenomena in strongly correlated electron systems, such as metal-insulator transition and anomalous transport properties [3].

The basic lattice structure of $R_2\text{Mo}_2\text{O}_7$ is composed of two intervening pyrochlore lattices: One is formed by Mo cations and the other is by R . The pyrochlore lattice is a three-dimensional network of corner-sharing tetrahedra, which is known to possess strong geometrical frustration. Mo cation is nominally tetravalent and has two electrons on average. The crystal field from trigonal distortion of MoO_6 octahedra splits three-fold t_{2g} levels of Mo $4d$ electrons into a_{1g} singlet and e'_g doublet. The trigonal axis is along the direction toward the center of each Mo tetrahedron, which is called the local $\langle 111 \rangle$ axis. With aligning their spins parallel according to the Hund's rule, one of two electrons occupies the lower a_{1g} level, and the other comes in the doubly-degenerate e'_g levels. (See, for example, Fig. 1 in Ref. [2].) Hence spin, charge, and

orbital degrees of freedom are all active in these compounds, and the frustration of the lattice structure promotes the competition among them by preventing a simple ordering. In addition, the coupling between Mo 4*d* electrons and *R*-site rare-earth moments brings about further complications. In the following, however, we will focus on the phenomena commonly observed regardless of magnetic or nonmagnetic *R* cations, such as the phase competition mentioned above, and neglect the *R* sites: We will concentrate on the Mo pyrochlore network alone and the intrinsic physics from Mo 4*d* electrons in this paper.

Several theoretical studies have been done for understanding the phase competition in the Mo pyrochlore oxides. A pioneering work was done for the chemical substitution at ambient pressure by Solovyev by using the LDA+*U* calculation [4]. The calculated electronic structure indicates that the lower *a*_{1*g*} level has rather localized nature with a narrow band, while the *e*'_{*g*} levels form a relatively wide band and bears itinerant nature. The observation suggests that the system can be viewed as a double-exchange (DE) system, in which localized *a*_{1*g*} spins are coupled with itinerant *e*'_{*g*} electrons via the ferromagnetic Hund's-rule coupling. This explains well the emergence of FM in the compounds with large ionic radius of *R*, such as *R*=Nd and Sm. The calculation while changing the value of *U* shows that the localization from FM to SG insulator by the substitution is basically understood by the correlation effect (or the bandwidth control). These calculations, however, were performed with assuming a simple collinear ferro or antiferromagnetic (AF) ordering; hence, the detailed nature of the frustrated insulating phase, such as the SG behavior and the orbital state, was not clarified.

Recently, the authors have studied the phase competition under applied pressure [5, 6, 7]. The results show that the change from FM, SG metal, to PM is well reproduced by Monte Carlo (MC) calculations for an extended DE model including the superexchange (SE) AF coupling between localized spins. In particular, the peculiar diffusive nature of PM is explained by the strongly incoherent state originating from competition between the DE ferromagnetic interaction and the SE AF interaction [5]. The SG metallic state is also accounted by an instability toward phase separation related to the competition [7]. The agreement implies that the physical pressure causes a different effect from the chemical pressure (chemical substitution), as implied in the experimental report [2]: The former tends to increase the SE AF coupling between the *a*_{1*g*} spins dominantly, while the latter mainly modifies the bandwidth of itinerant *e*'_{*g*} electrons. MC calculations so far were performed for a single-band model with neglecting the Coulomb repulsion between itinerant electrons; for comprehensive understanding of the phase competition in the Mo pyrochlore oxides, it is necessary to extend the analysis to incorporate the electron correlation as well as the *e*'_{*g*} orbital degree of freedom.

In this contribution, we investigate the effect of electron correlation and orbital degeneracy on the phase competition in the extended DE model. The model explicitly includes the twofold orbital degeneracy and the Coulomb repulsion between itinerant electrons. Thermodynamic properties of the model are studied by MC calculations, in which the electron correlation is handled by an unrestricted-type Hartree approximation. The results indicate that, in addition to the phase transition from FM to PM previously obtained in the single-band model, a metal-insulator transition is caused by the electronic correlation accompanied by a 'ferro'-type orbital ordering. We discuss the phase diagram in relation to the distinct behaviors in experiments for the chemical substitution and the applied pressure in the Mo pyrochlore oxides.

2. Model and method

As an extension of the previous studies [5, 6, 7], we here consider the DE model with twofold orbital degeneracy. The Hamiltonian is given by

$$\mathcal{H} = \sum_{\langle ij \rangle} \sum_{\alpha\beta} \sum_{\sigma} t_{\alpha\beta} (c_{i\alpha\sigma}^{\dagger} c_{j\beta\sigma} + \text{H.c.}) + \frac{1}{2} \sum_i \sum_{\alpha\beta\alpha'\beta'} \sum_{\sigma\sigma'} U_{\alpha\beta\alpha'\beta'} c_{i\alpha\sigma}^{\dagger} c_{i\beta\sigma'}^{\dagger} c_{i\beta'\sigma'} c_{i\alpha'\sigma}$$

$$-J_H \sum_i \sum_{\alpha} c_{i\alpha\sigma}^{\dagger} \vec{\sigma}_{\sigma\sigma'} c_{i\alpha\sigma'} \cdot \vec{S}_i + J_{AF} \sum_{\langle ij \rangle} \vec{S}_i \cdot \vec{S}_j, \quad (1)$$

where $c_{i\alpha\sigma}^{\dagger}$ ($c_{i\alpha\sigma}$) creates (annihilates) an electron with orbital α and spin σ at site i , $\vec{\sigma}$ denotes the Pauli matrix, and \vec{S}_i represents the localized spin at site i . The first term describes the electron hopping between nearest-neighbor sites $\langle ij \rangle$ on the pyrochlore lattice; the transfer integrals depend on the orbital indices α and β which represent two e'_g orbitals. The second term denotes the onsite Coulomb interactions between the e'_g electrons, including the intra and interorbital repulsions, the Hund's-rule coupling, and the pair hopping. The third term denotes the Hund's-rule coupling between itinerant electrons and localized spins \vec{S}_i . The last term is the SE AF coupling between the neighboring localized spins. A similar model has been studied on the square or cubic lattices in the context of colossal magnetoresistive (CMR) manganites [8].

Our purpose is to clarify thermodynamics of the model given by Eq. (1) and to elucidate the competing phases including correlated disordered states, such as the diffusive PM or the Mott insulating state. For this purpose, some sophisticated method beyond a simple mean-field approximation is necessary. The model (1), however, is very complicated and difficult to handle beyond a simple mean-field approximation. Hence, we introduce several simplifications as follows. First we take the limit of large J_H . In this limit, as often considered in the study of CMR, spins of itinerant electrons are aligned parallel to the localized spin at each site, and the transfer integrals are modulated by the relative angle between the neighboring localized spins. At the same time, among many contributions in the second term in Eq. (1), only the interorbital interaction between the same spin electrons remains relevant. Furthermore, we consider the localized spins \vec{S}_i as classical vectors with the renormalized length $|\vec{S}_i| = 1$. The simplifications were shown to give reasonable results in the study of a single-band model for the phase competition under pressure in the wide-bandwidth compounds [5, 6, 7]. Consequently, by taking the local spin axis along the direction of localized spin at each site, the model can be described by spinless fermions in the form

$$\mathcal{H} = \sum_{\langle ij \rangle} \sum_{\alpha\beta} \tilde{t}_{i\alpha j\beta} (\tilde{c}_{i\alpha}^{\dagger} \tilde{c}_{j\beta} + \text{H.c.}) + \frac{\tilde{U}}{2} \sum_i \sum_{\alpha \neq \beta} \tilde{n}_{i\alpha} \tilde{n}_{i\beta} + J_{AF} \sum_{\langle ij \rangle} \vec{S}_i \cdot \vec{S}_j, \quad (2)$$

where $\tilde{c}_{i\alpha}$ is the spinless fermion operator and $\tilde{n}_{i\alpha} = \tilde{c}_{i\alpha}^{\dagger} \tilde{c}_{i\alpha}$. Here, \tilde{U} is considered as an effective interorbital interaction, which controls the double occupancy in the e'_g orbital with the same spin electrons under the strong Hund's-rule coupling; its origin is traced back to the e'_g interorbital Coulomb repulsion and the Hund's-rule couplings between e'_g - e'_g and e'_g - a_{1g} orbitals in Eq. (1). Hereafter, we consider the filling with one electron per site on average.

In Eq. (2), the effective transfer integral is given by

$$\tilde{t}_{i\alpha j\beta} = t_{\alpha\beta} \left[\cos \frac{\theta_i}{2} \cos \frac{\theta_j}{2} + \sin \frac{\theta_i}{2} \sin \frac{\theta_j}{2} \exp\{-i(\phi_i - \phi_j)\} \right], \quad (3)$$

where (θ_i, ϕ_i) denotes the angle of \vec{S}_i . To estimate the value of $t_{\alpha\beta}$, it is necessary to take account of the anisotropy of the e'_g orbitals and the relative angle of Mo-O-Mo bond. Following the calculation in Ref. [9], we estimate the orbital diagonal and off-diagonal elements: it turns out that the ratio between them depends solely on the Mo-O-Mo bond angle δ as

$$\frac{t_{\alpha \neq \beta}}{t_{\alpha = \beta}} = \frac{3 - \cos \delta}{3 + \cos \delta}. \quad (4)$$

Thus, the orbital off-diagonal element is larger than the diagonal one for $\delta > 90^\circ$. In Mo pyrochlore oxides, δ is estimated around 130° at ambient pressure [10]. In the following

calculations, for simplicity, we consider only the dominant off-diagonal element and fix $t_{\alpha \neq \beta} = -1$ and $t_{\alpha=\beta} = 0$, although the transfer integrals might change depending on both chemical and physical pressure.

We study the model (2) by MC simulation in a similar way as in the previous studies for the single-band model [5, 6, 7]. To facilitate the MC calculations without negative sign problem, we introduce an unrestricted-type mean-field decoupling to the Coulomb interaction in the second term in Eq. (2). Here, as the simplest approximation, we employ the Hartree approximation; $\tilde{n}_{i\alpha}\tilde{n}_{i\beta} \rightarrow \langle \tilde{n}_{i\alpha} \rangle \tilde{n}_{i\beta} + \tilde{n}_{i\alpha} \langle \tilde{n}_{i\beta} \rangle - \langle \tilde{n}_{i\alpha} \rangle \langle \tilde{n}_{i\beta} \rangle$. The MC sampling is performed to update the configurations of localized spins $\{\vec{S}_i\}$. In each MC step, the mean fields $\{\langle n_{i\alpha} \rangle\}$ are recalculated by using the eigenvalues and eigenvectors obtained from the exact diagonalization of the Hamiltonian (2). We confirmed the convergence of the mean fields within the statistical errorbars after thermalization. We also employ the averaging over the twisted boundary conditions to suppress the finite size effect [6]. In the following, we show the result for 16 site system with averaging over 8^3 different twisted boundary conditions. Typically, we perform 2000 MC steps for measurement after 1000 MC steps for thermalization.

3. Result

Figure 1 shows the MC results for the model (2) at a low temperature $T = 0.04$ while changing the Coulomb repulsion \tilde{U} and the SE AF coupling J_{AF} . We compute the square of magnetization m^2 , the charge compressibility χ_c , and the z component of orbital polarization τ^z , by

$$m^2 = \left\langle \left(\frac{1}{N_s} \sum_i \vec{S}_i \right)^2 \right\rangle, \quad (5)$$

$$\chi_c = \frac{\partial \langle \tilde{n} \rangle}{\partial \mu} = \frac{\partial}{\partial \mu} \left\langle \frac{1}{N_s} \sum_{i\alpha} \tilde{n}_{i\alpha} \right\rangle, \quad (6)$$

$$\tau^z = \left\langle \left| \frac{1}{N_s} \sum_i (\tilde{n}_{i\alpha} - \tilde{n}_{i\beta}) \right| \right\rangle, \quad (7)$$

respectively. Here the bracket $\langle \cdots \rangle$ denotes the thermal average, N_s is the number of sites, μ is the chemical potential, and \tilde{n} is the electron density.

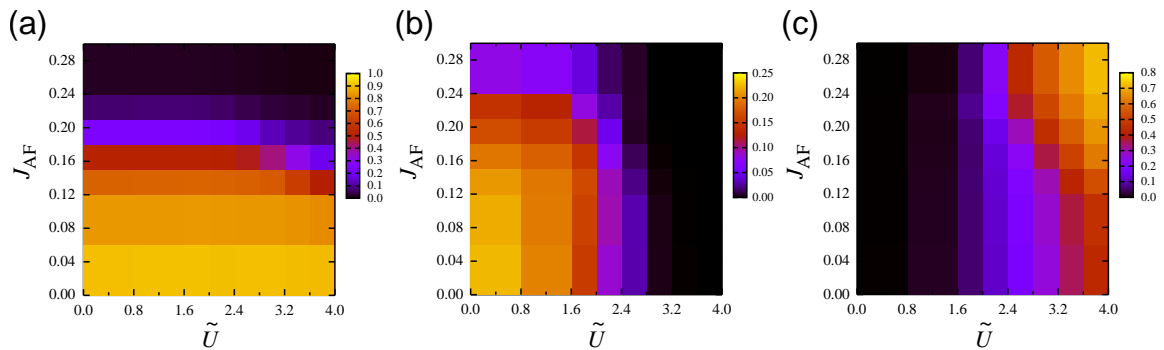


Figure 1. MC results for the model given by Eq. (2) at $\langle \tilde{n} \rangle = 1$ and $T = 0.04$: (a) square of the magnetization m^2 [Eq. (5)], (b) charge compressibility χ_c [Eq. (6)], and (c) z component of orbital polarization τ^z [Eq. (7)]. The results are obtained for 16 site cluster by taking average over twisted boundary conditions with 8^3 different fluxes.

As shown in Fig. 1(a), in the small J_{AF} region, the magnetization is large, indicating that the system is ferromagnetic. The ferromagnetism collapses as J_{AF} increases. On the other hand,

the magnetism is relatively insensitive to \tilde{U} . For small \tilde{U} , the charge compressibility χ_c is finite as shown in Fig. 1(b), indicating that the system is metallic. Hence, the system is FM for small J_{AF} , while it turns into PM as J_{AF} increases in the small \tilde{U} region. This behavior is qualitatively the same as observed in the single-band model [5]. In the single-band case, phase separation appears between the two phases [7]; we expect a similar behavior in the present two-band case, but it is not clearly seen in the present calculation presumably because of the small size cluster.

As \tilde{U} increases, χ_c decreases rapidly to zero, as shown in Fig. 1(b). This signals the metal-to-insulator transition. The insulating state is characterized by an orbital ordering. Figure 1(c) shows that the orbital polarization becomes nonzero almost simultaneously with the disappearance of the charge compressibility. This means that the insulating state shows a ‘ferro’-type orbital order by choosing one of two e'_g orbitals. The reason for the ‘ferro’-type orbital order is understood from the strong coupling picture as follows. In the large \tilde{U} limit, the second order perturbation in the transfer integrals leads to the so-called Kugel-Khomskii-type spin-orbital exchange couplings [11]. In the present model, as seen in Fig. 1(a), the spin configuration is governed by the competition between DE and SE interactions, not by \tilde{U} . Then, the ‘ferro’-type orbital configuration is favored via the spin-orbital exchange couplings, irrespective of spin configurations, because the dominant hopping processes in the perturbation are the orbital off-diagonal ones by $t_{\alpha\neq\beta}$ in the present model. The situation is contrastive to the ‘myth’ for the Kugel-Khomskii-type interactions, in which the system usually favors complementary spin-orbital configurations, such as spin-AF orbital-ferro or spin-ferro orbital-AF.

It is worthy to note that the ‘ferro’-type orbital order is not a uniform orbital order. The trigonal distortion is along the local $\langle 111 \rangle$ axis at each site, and hence, the e'_g orbital polarization takes place along the site-dependent local axis. In other words, the ‘ferro’-type orbital order is a $\vec{q} = 0$ four-sublattice order. Thus it does not break the cubic symmetry of the pyrochlore lattice structure.

Summarizing the results, we obtain four dominant phases at low temperatures in the plane of \tilde{U} and J_{AF} , as schematically shown in Fig. 2. The spin-ferro orbital-para metal in the small \tilde{U} and small J_{AF} region is stabilized by the DE mechanism. The spin-para orbital-para metal in the small \tilde{U} and large J_{AF} region is induced by the competition between the DE ferromagnetic interaction and the SE AF coupling under the geometrical frustration. In these two phases, the orbital degree of freedom is less important, and hence, the physics is common to the single-band case [5, 6, 7]. On the other hand, the spin-ferro and orbital-‘ferro’ insulator in the large \tilde{U} and small J_{AF} region is a correlation-driven insulator with development of the orbital ordering. The spin-para orbital-‘ferro’ insulator is driven by the increase of J_{AF} and the spin frustration.

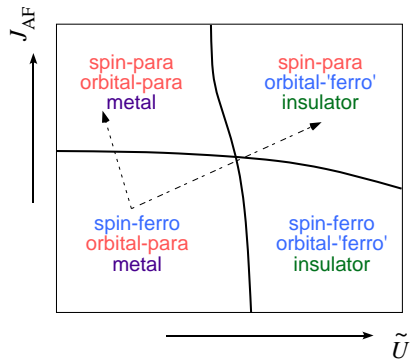


Figure 2. Schematic phase diagram at low temperatures suggested from the results in Fig. 1. The dotted (dot-dashed) arrow in the figure indicates a possible parameter change while changing the physical (chemical) pressure in the Mo pyrochlore oxides. See the text for details.

4. Discussion and concluding remark

In Mo pyrochlore oxides, as mentioned in Sec. 1, the chemical substitution leads to the transition from FM to SG insulator, while the pressure induces the transition from FM to PM. The latter

is qualitatively explained by the change of J_{AF} in the single-band model [5], and the present calculation for the extended two-band model also gives similar results in the small \tilde{U} regime; the parameter change is, e.g., schematically shown by the dotted arrow in Fig. 2. On the other hand, the metal-insulator transition by the chemical substitution cannot be understood by the single-band physics. From our results, we deduce that the transition from FM to SG insulator is described by the transition from the spin-ferro orbital-para metal to the spin-para orbital-‘ferro’ insulator, as indicated by the dot-dashed arrow in Fig. 2. In the spin-para orbital-‘ferro’ insulating state, the spin degree of freedom remains paramagnetic because of the strong frustration, but short-range AF correlations are expected by the dominant J_{AF} . The remaining frustration might be released by remnant perturbations neglected in the present model. In fact, one of the author and his collaborators recently demonstrated that the frustrated spins have instability toward a SG state through the coupling to local lattice distortions in the presence of bond disorder, reasonably in accord with the experiments in Mo pyrochlore oxides [12]. Thus, our results provide a hint for understanding the nature of the frustrated Mott insulating state in the Mo pyrochlore oxides. From these observations, we consider that, despite several simplifications introduced, our effective two-band model given by Eq. (2) can offer a simple starting point for comprehensively understanding the intricate physics $R_2\text{Mo}_2\text{O}_7$. Further analysis in larger system sizes is desired to elucidate the thermodynamics as well as transport properties.

Why and how the two effects, the chemical substitution and the pressure, lead to such different behaviors remain unclear. In the present scenario, these effects are attributed to the different control of the Coulomb repulsion (or the bandwidth) and the SE AF coupling between a_{1g} spins. The bandwidth is basically determined by the transfer integrals between the itinerant e'_g orbitals, i.e., $t_{\alpha\beta}$ in our model, on the other hand, the SE AF coupling J_{AF} is approximately set by $t_{a_{1g}}^2/U_{a_{1g}}$, where $t_{a_{1g}}$ and $U_{a_{1g}}$ are the transfer integral between the a_{1g} orbitals and the intraorbital Coulomb repulsion in the a_{1g} orbital, respectively. Both $t_{\alpha\beta}$ and $t_{a_{1g}}$ are modified by the chemical or physical pressure via the change of the angle and/or bond length of Mo-O-Mo bonds. In order to clarify how they are modified and to distinguish the two effects, it is highly desired to study the microscopic change of the lattice parameters by, e.g., the detailed x-ray scattering experiment or the first-principles calculations with structural optimization.

The authors thank Y. Tokura, S. Iguchi, and H. Shinaoka for fruitful discussions. This work was supported by Grant-in-Aids (Nos. 19052008 and 21340090), Global COE Program “the Physical Sciences Frontier”, and the Next Generation Super Computing Project, Nanoscience Program, MEXT, Japan.

References

- [1] Greedan J E, Sato M, Ali N and Datars W R 1987 *J. Solid State Chem.* **68** 300
- [2] Iguchi S, Hanasaki N, Kinuhara M, Takeshita N, Terakura C, Taguchi Y, Takagi H and Tokura Y 2009 *Phys. Rev. Lett.* **102** 136407
- [3] For a recent review, see Gardner J S, Gingras M J P and Greedan J E 2010 *Rev. Mod. Phys.* **82** 53
- [4] Solovyev I V 2003 *Phys. Rev. B* **67** 174406
- [5] Motome Y and Furukawa N 2010 *Phys. Rev. Lett.* **104** 106407
- [6] Motome Y and Furukawa N 2010 *J. Phys.: Conf. Ser.* **200** 012131
- [7] Motome Y and Furukawa N 2010 *Phys. Rev. B* **82** 060407(R)
- [8] For a review, see Dagotto E, Hotta T and Moreo A 2001 *Phys. Rep.* **344** 1
- [9] Ichikawa H, Kano L, Saitoh M, Miyahara S, Furukawa N, Akimitsu J, Yokoo T, Matsumura T, Takeda M and Hirota K 2005 *J. Phys. Soc. Jpn.* **74** 1020
- [10] Moritomo Y, Xu Sh, Machida A, Katsufuji T, Nishibori E, Takata M, Sakata M, and Cheong S-W 2001 *Phys. Rev. B* **63** 144425
- [11] Kugel K I and Khomskii D I 1973 *Zh. Eksp. Teor. Fiz.* **64** 1429 [*Sov. Phys. JETP* **37** 725]
- [12] Shinaoka H, Tomita Y and Motome Y 2010 Spin-glass transition in bond-disordered Heisenberg antiferromagnets coupled with local lattice distortions on a pyrochlore lattice *Preprint* arXiv:1010.5625